

AN EXPERIMENTAL STUDY ON THE BLEEDING OF FRESH CONCRETE IN STATIC AND VIBRATED STATES

Wenbo ZHANG^{*1}, Zhuguo LI^{*2}, and Jieyong LI^{*3}

ABSTRACT

The effects of specimen's dimensions, and other factors, such as water-cement ratio, on bleeding of fresh concrete in static and vibrated states are experimentally investigated, respectively. Then, a model is presented to describe the time-dependence of bleeding capacity, and the quantitative relationships between the parameters in the model and various influencing factors are examined. Also, the variation of bleeding rate with pore water pressure is discussed. Moreover, it is observed that final bleeding volume in static state can be predicted by the total bleeding during the 5 minutes vibration.

Keywords: bleeding, fresh concrete, influencing factors, pore water pressure, time-dependent model

1. INTRODUCTION

Some bleeding is normal for good concrete; it results in a film of water over the entire surface preventing drying out prior to hydration. Excessive bleeding would damage the concrete structure, generating weak zones, reducing bond, and inducing anisotropy of strength of up and down concrete, and lead to laitance, and plastic shrinkage cracks, etc. on concrete's surface. Therefore, many studies have been performed on the influencing factors of concrete bleeding. Bleed water tends to occur more in concretes that have: retarded setting, low cement content, high water-cement ratio, coarse ground cement or poorly graded aggregates [1]. Burak et al. [2] have proposed that optimum water-cement ratio for producing self-compacting concrete (SCC) is in the range of 0.84-1.07 by volume. In addition, a study represented that the species of fine aggregate also have an effect on the bleeding properties [3]. Though many investigations on the effects of materials and mix proportions on bleeding of concrete have been performed, almost all these investigations are qualitative ones, and only a few examinations of the effects of specimen's dimensions were made.

It is thought that the bleeding mainly results from the particle (aggregates) consolidation [4]. The settlement of the solid particles causes higher pore water pressure in lower part of the sample and bleeding channels [5]. Accordingly, an increase in the pore water pressure could result in the bleeding. But the relationship between bleeding rate and excessive pore water pressure is not yet clarified, which would be used to predict the bleeding capacity of concrete.

When evaporation rate of water from a concrete's surface is more than a value, e.g. $0.5\text{kg/m}^2\cdot\text{h}$ [6], the concrete would be in danger of early dry shrinkage cracks. This limit value depends on temperature,

humidity, and wind velocity, etc. Obviously, adequate bleeding may help prevent the early shrinkage cracks. Hence, the prediction of bleeding rate is necessary.

For casting concrete in mould, appropriate vibration is necessary. However, the vibration would lead to the settlement of aggregates, and accelerate the bleeding. Standard bleeding test can evaluate the segregation resistance of the mixing water in static fresh concrete, but can't express the bleeding capacity of vibrated concrete in construction site. For predicting the bleeding capacity of vibrated concrete based on the result of the standard bleeding test, it is necessary to investigate the relationship between the bleeding capacities of static and vibrated states, as well as the effects of concrete dimensions on this relationship.

In this study, first, the effects of various factors on bleeding, including specimen's thickness and surface area, vertical pressure on the top of concrete, and mix proportions, are experimentally examined. Then, a model is proposed to describe time-dependence of the bleeding, and quantitatively discuss the effects of various factors mentioned just above on the parameters of the model. Also, the relationships between the bleeding rate and pore water pressure in static and vibration states are investigated respectively. Moreover, a series of bleeding tests are carried out to respectively examine the bleeding capacities during vibration and after the vibration. The relationships between the quantities of bleed water during 5-minutes vibration, whole process of vibration plus standstill, and the bleeding volume obtained by the standard bleeding test are also investigated quantitatively for developing methods of predicting the bleeding capacity of vibrated concrete in construction site, and estimating the bleeding in the whole casting process by a short and simple approach.

2. EXPERIMENTAL PROGRAMS

*1 Graduate Student, Graduate School of Science and Engineering, Yamaguchi University, JCI Member

*2 Associate Professor, Graduate School of Science and Engineering, Yamaguchi University, JCI Member

*3 Graduate Student, Graduate School of Science and Engineering, Yamaguchi University, JCI Member

2.1 Raw Materials and Mix Proportions of Concrete

The concrete mixes used in this study were prepared with ordinary portland cement, sea sand, and crushed stone. The characteristics of sea sand and crushed stone are shown in Table 1. Standard as well as Air-entraining (AE) plasticizer or AE super-plasticizer were also used in the concretes.

The mixing procedure of the concretes is: mix firstly the fine aggregate and cement for 60s before adding the mixing water and the admixture to mix the mortar for 96s. Finally, add the coarse aggregate and mix for 144s to produce the desired concretes. The slump, slump flow, 50cm-flow time, and unit mass of freshly mixed concrete were measured, respectively. Table 2 summarizes the mix proportions, and the properties in fresh state.

2.2 Test Method

Bleeding tests in static state were performed following the standard method of JIS A1123, using a standard cylindrical container with 250mm diameter and 285mm depth. The bleed water was sucked up every 10 minutes in the first one hour, and then at an interval of 30 minutes one hour later. However, when applying a vertical pressure on the surface of concrete specimen, we sucked up once at every 5 minutes in the first hour and then at an interval of 10 minutes. When fresh concrete was vibrated for 5 minutes on a vibration table, the bleeding water was sucked up at 30-second intervals in the first 5 minutes, and then at 5 minutes intervals for an hour. Pore water pressures in concrete specimens, including hydrostatic pressure in static state and excessive pore water pressure in vibrated state, were measured by water-pressure gauges (Model BPR-A-50KPS), which were fixed on the inner surface of the used container at 5cm height from the bottom.

Table 1 Characteristics of the aggregates used

Property	Type of aggregate	
	Sea sand	Crushed stone
Density in water-saturated state (g/cm ³)	2.59	2.73
Absorption ratio (%)	1.60	0.40
Fineness modulus	2.57	6.67
Maximum size (mm)	5	20

The bleeding capacity, bleeding ratio, and bleeding rate are expressed with Eqs.1-3, respectively.

$$B_q = V / A \quad (1)$$

$$B_r = \frac{V}{10Q_c \times W} \% \quad (2)$$

$$\nu = \Delta B_q / \Delta t \quad (3)$$

where B_q is bleeding capacity (cm³/cm²), B_r is bleeding ratio, ν is bleeding rate (cm³/cm²/min), V is final quantity of bleed water (ml), A is surface area of concrete specimen (cm²), Q_c is volume of tested concrete (m³); W is water content (kg/m³), ΔB_q (cm³/cm²) is an increase of bleeding capacity at Δt interval (min).

3. RESULTS AND DISCUSSION

3.1 Effects of Specimen's Dimensions on the Bleeding in Static State and Vibration

These investigations were carried out, using concrete specimens of series C1, C2, C3 and C14, which have fluidity of a wide range from lower to higher one. Fig. 1 shows the variation of bleeding with elapsed time, and the effects of the specimen's

Table 2 Mix proportions and fluidity of used concretes

Series	Mix proportions		Unit mass (kg/cm ³)					Properties of fresh concrete			
	W/C (%)	S/a (%)	W	C	S	G	Sp (C×%, by mass)	Sl. (cm)	Sf. (mm)	T ₅₀ (s)	ρ (kg/m ³)
C1	50	38	165	330	691	1128	0.4*	8.1	-	-	2400
C2	50	40	170	340	718	1077	0.8*	15.0	-	-	2359
C3	50	42	185	370	726	1002	1.0**	26.2	630	1.58	2410
C4	50	38	165	330	691	1128	0.8**	25.1	456	-	2438
C5	50	38	175	346	678	1106	0.9**	24.0	502	4.39	2420
C6	50	38	183	366	661	1079	0.8**	26.6	623	2.62	2414
C7	40	38	183	458	633	1032	0.8**	25.5	580	3.75	2430
C8	45	38	183	407	648	1058	0.8**	24.3	594	2.39	2421
C9	55	38	183	333	672	1096	0.8**	24.1	562	3.00	2430
C10	50	36	175	350	640	1138	0.9**	25.3	570	2.02	2364
C11	50	41	175	350	726	1045	0.9**	24.7	538	4.31	2244
C12	50	44	175	350	778	990	0.9**	24.1	480	-	2383
C13	50	38	165	330	691	1128	0.4**	9.0	-	-	2417
							1.2**	23.0	602	3.98	2436
							1.6**	24.6	613	3.48	2437
C14	50	38	175	350	674	1100	0.8*	18.2	-	-	2330

[Notes] W/C: Water-cement ratio; S/a: Sand-aggregate mass ratio; W, C, S and G: Mass of water, cement, sand, and gravel in 1m³ concrete, respectively (kg); Sp*: Air Entrained plasticizer; Sp**: Air Entrained super-plasticizer; Sl.: Slump; T₅₀: 50cm-flow time; Sf.: Slump flow; and ρ: unit mass of concrete.

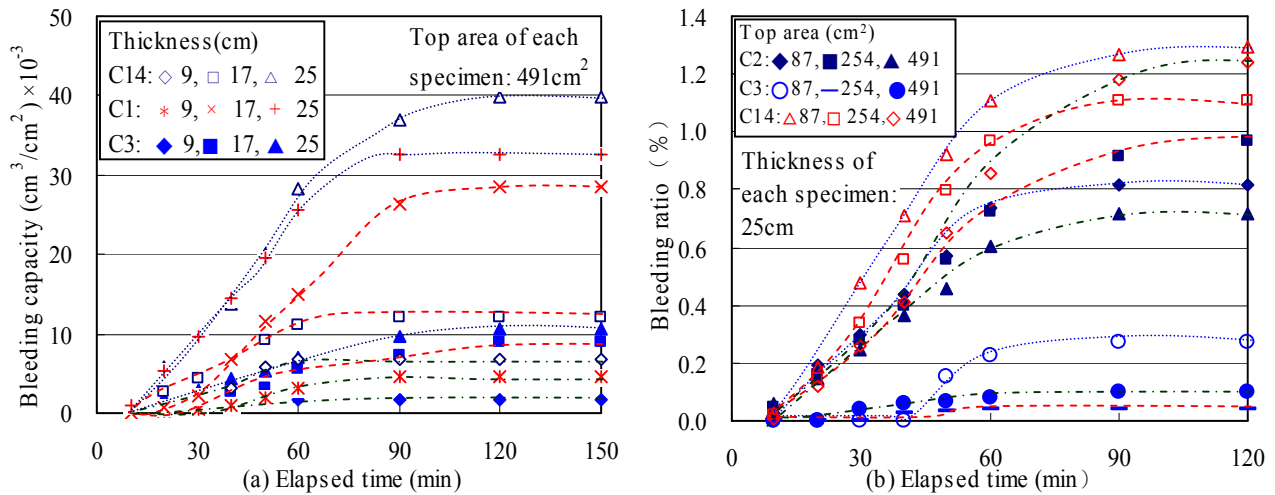


Fig. 1 Variation of bleeding capacity and bleeding ratio with elapsed time in static state

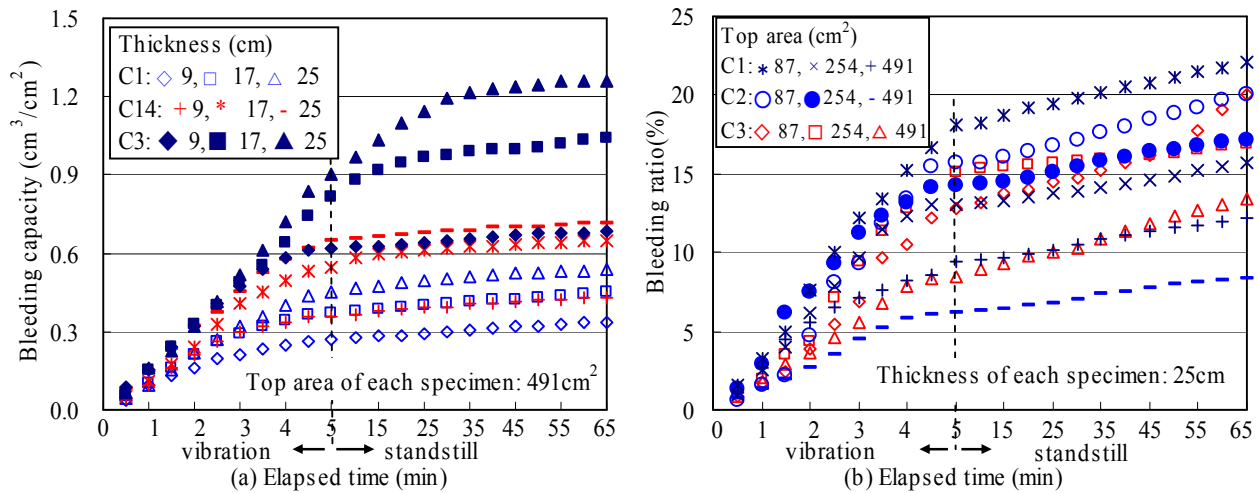


Fig. 2 Variation of bleeding capacity and bleeding ratio with elapsed time in vibration state

thickness and top area on this time-dependence.

As shown in Fig. 1(a), the bleeding capacity increased with the thickness of specimen for any kind of concrete. This probably attributes to that the thicker the specimen, the greater the content of mixing water, and thus quantity of bleed water becomes greater. Also, thicker specimen yields a relatively greater pore pressure to the concrete in the lower part, thus the bleed water may occurs easily. On the other hand, Fig. 1(a) also shows that for the same thickness of different specimen, the bleeding capacity of the high fluidity concrete was smaller than that of the low and middle fluidity concretes. This is because the use of many AE super-plasticizer made the cohesiveness of high fluidity concrete greater.

Fig. 1(b) indicates the effect of specimen's top area on the bleeding ratio. The bleeding ratio of series C3, which is high fluidity concrete mixed a lot of AE super-plasticizer, is lower than that of low or middle fluidity concretes. For any series of concrete, the bleeding ratio of specimen is in the order of top area 87, 491 and 254 cm^2 . That is to say, moderate top area yields the smallest bleeding ratio, and the specimen with smaller top area would have the greatest quantity of bleed water. A lot of bleed water rises up to the concrete surface along the inner surface of the container.

Hence, the greater the specific lateral surface area, the larger the area that the specimen contacts to the inner-surface of the container. Smaller top area will result in a greater specific lateral surface area of specimen; accordingly the bleeding ratio is greater. However, some of bleed water goes up through water channels in specimen. The greater the top surface area, the more the water channels. Hence, the specimen with larger section has more bleed water.

Fig. 2 indicates the test results of bleeding for 4 kinds of fluidity of vibrated fresh concretes, which had different heights and top areas. It is observed that there was a rapid increase in bleeding capacity or bleeding ratio during the vibrated stage. After vibrated, the bleeding continued to occur during the static state. The total bleeding capacity during the whole process of vibration plus standstill increased with increasing specimen's height (Fig. 2(a)), while the bleeding ratio decreased as the top area increased (Fig. 2(b)). This is probably because the volume of specimen having greater top area was greater; this made the subjected vibration energy of the specimen of unit volume smaller. We can also find that the high fluidity concrete had more total bleeding capacity for the same specimen height (Fig. 2(a)). When the specimen's height turns

Table 3 Values of coefficient V in the equation

Influencing factors	Fluidity	V	
Specimen's thickness (h , cm)	Low (C1)	$V = 0.8836h - 3.9270$	$R^2 = 0.856$
	Middle (C14)	$V = 1.3084h - 7.7067$	$R^2 = 0.866$
	High (C3)	$V = 0.2945h - 1.2272$	$R^2 = 0.881$
Specimen's top surface area (A , cm ²)	Low (C1)	$V = 0.0006A^2 + 0.0145A$	$R^2 = 0.277$
	Middle (C14)	$V = -3E-06A^2 + 0.0540A$	$R^2 = 0.025$
	High (C3)	$V = -0.0001A^2 + 0.0109A$	$R^2 = 0.296$
Vertical pressure on specimen's top surface (σ_v , Pa)	Low (C2)	$V = 11.8301\sigma_v + 10.7501$	$R^2 = 0.966$
	Middle (C14)	$V = 5.9396\sigma_v + 64.7463$	$R^2 = 0.849$
	High (C3)	$V = 4.1724\sigma_v + 93.8060$	$R^2 = 0.986$
Sp (g)	-	$V_0 = 1510.664Sp + 8.7376$	$R^2 = 0.992$
VMA (g/m ³)	-	$V_0 = -0.1964VMA + 130.82$	$R^2 = 0.997$
S/a (%)	-	$V_0 = -304.980S/a + 148.882$	$R^2 = 0.957$
W (kg/m ³)	-	$V_0 = 0.6381W - 65.630$	$R^2 = 0.803$
W/C (%)	-	$V_0 = 1.8162W/C - 55.6161$	$R^2 = 0.931$

Note: VMA: Dosage of viscosity modifying agent, V_0 : Final bleed water volume measured with the standard specimen container

into greater, the water content in the concrete specimen will be larger. Therefore, under vibration, there will be more bleed water from the specimen. Furthermore, as shown in Fig. 2(b), for the same top surface area (254 or 491 cm²), the higher the fluidity of concrete, the greater the total bleeding ratio under the vibration.

3.2 Quantitative Relationships between Bleeding Quantity and Various Influencing Factors

Besides the specimen dimensions, the effects of many other influencing factors, including vertical pressure on the top surface of the specimens, water-cement ratio, unit water content, fine aggregate ratio, and admixture content, etc., on the bleeding capacity in static state were also investigated experimentally. The tendency of variation of bleeding capacity with elapsed time under various conditions was the same as shown in Fig. 1(a). Due to the limitation of space, the figures of experimental results are not given here. We describe approximately this time-dependence with the Eq. 4 according to Fig. 1(a).

$$[B_q]_t = \frac{V}{A} [1 - \exp(-\frac{Vt}{10Q_c W} \%)] \quad (4)$$

where $[B_q]_t$ is bleeding capacity (cm³/cm²) at any elapsed time t , V is final quantity of bleed water (cm³).

By a series of regression analyses, we obtained the relational formulas between the final bleed water volume and various factors, as shown in Table 3. Also, we examined the relational formula between the final bleed water volumes (V_0 , V) measured with the standard specimen container (diameter: 25cm, depth 28.5cm) and non-standard specimen container, as shown in Eq.5.

$$V = V_0(0.002A + 0.051h), R^2 = 0.808 \quad (5)$$

After the final bleed water volume V_0 is measured by the standard method JIS A1123, we can predict the bleeding capacity of concrete with actual dimensions (A ,

h) at any time based on Eqs. 4-5, and further calculate the bleeding rate by Eq.3. Comparing bleeding rate with evaporation rate of water may help us judge whether spray curing is necessary for avoiding the early dry shrinkage cracks.

3.3 Relationships between Bleeding Quantities in the Static and Vibrated States

Besides specimen dimensions, W/C ratio, unit water content, fine aggregate ratio, and dosages of admixtures, etc., were changed to do series of bleeding tests under vibrated and static states. The concrete used are the same as the bleeding tests in standstill state, shown in Table 2. We measured the bleeding capacities, occurring during the vibration of 5 minutes,

and during the vibration of 5 minutes and 1 hour standstill after vibrated, respectively. Fig. 2 shows an example. Due to the limitation of space, variations of bleeding capacity under various conditions with time are not expressed with figures here, but the test results are shown in Fig. 3.

Fig. 3 shows the relationships between bleeding volumes of bleeding test in standstill (V_1), 5-minute vibration (V_2), and 5-minute vibration plus standstill (V_3). From this figure, we can see that the greater the bleeding volume V_1 in standstill state, the greater the V_2 and the V_3 . Two relational expressions were obtained by the linear regression analyses, as shown in Eqs. 6 and 7.

$$V_1 = 0.35V_2 - 52.07, R^2 = 0.512 \quad (6)$$

$$V_3 = 5.15V_1 + 152.97, R^2 = 0.666 \quad (7)$$

By using Eq. 6, we can predict the final bleeding capacity in standstill though measuring the bleed water during the 5-minute vibration, and by Eq. 7, bleeding

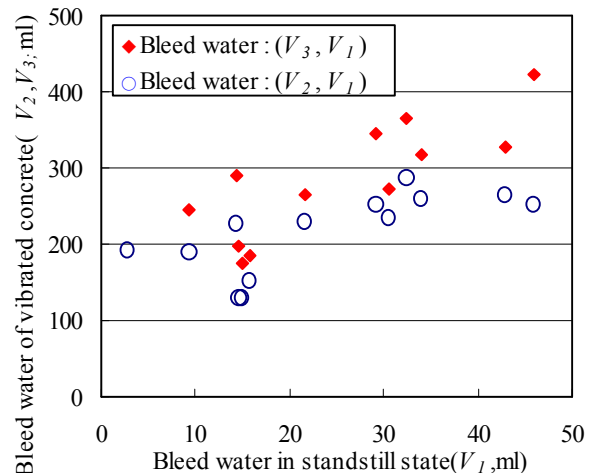


Fig. 3 Relationships between the bleeding quantities in static and vibrated states

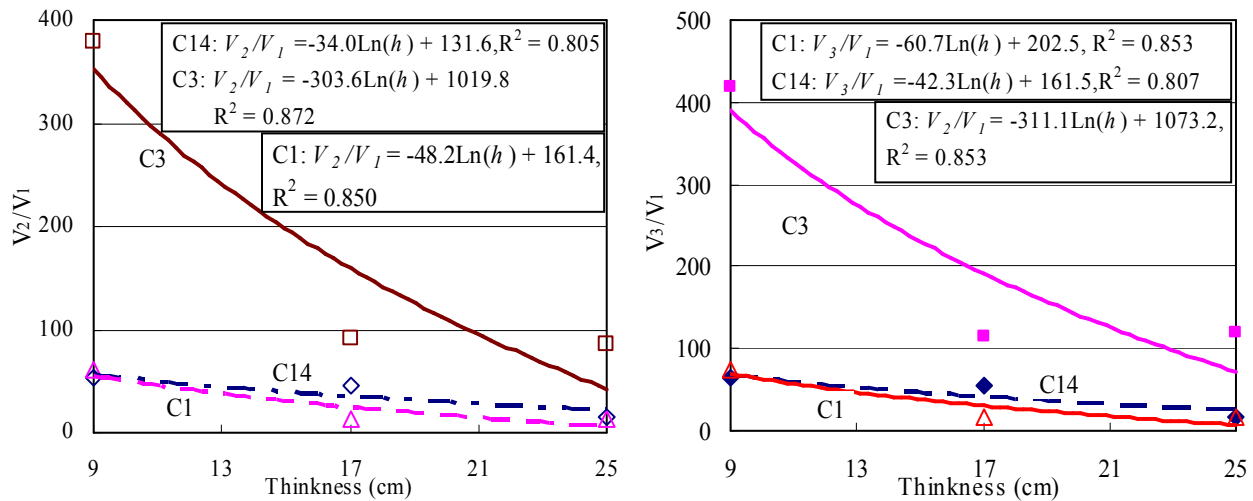


Fig. 4 Effects of specimen's height on the V_2/V_1 and V_3/V_1

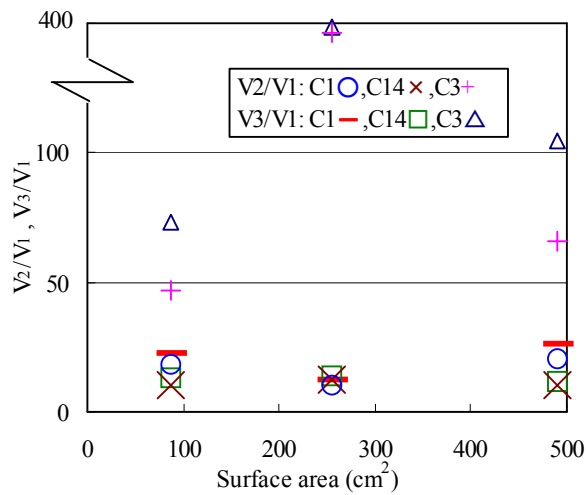


Fig. 5 Effects of surface area on the V_2/V_1 and V_3/V_1

capacity of vibrated concrete would be estimated.

The effects of specimen's dimensions (height and section surface area) on the V_2/V_1 and the V_3/V_1 were investigated for three levels of fluidity, as shown in Figs. 4 and 5. Fig. 4 indicates that the V_2/V_1 and the V_3/V_1 decreased with increasing specimen's thickness. This is because the thicker the specimen, the smaller the vibration energy applied to the specimen of unit volume, for the same concrete and section surface area. The relational formulas of V_2/V_1 , V_3/V_1 and concrete's thickness (h , cm) were obtained as shown in Fig. 4. However, we cannot find the two ratios correlated closely with the section surface area from Fig. 5.

3.4 Relationships between Pore Water Pressure and Bleeding Rate in Static and Vibrated States

Variations of hydrostatic pressure and bleeding rate with elapsed time, and the relationship between hydrostatic pressure and bleeding rate in standstill are shown in Fig. 6 for concrete C13 using different dosages of AE super-plasticizer. The bleeding rate and hydrostatic pressure rapidly increased with time right after the concrete was filled into the container, the former decreased with time, but the latter decreases or kept at a stable value, after they reached to their each

maximum value (Fig. 6(a)). The increase of hydrostatic pressure was probably resulted from the gravity of specimen and the sedimentation of aggregates around the water-pressure gauge. Though the measured water pressure is called as hydrostatic pressure, it might include excessive pore water pressure. As shown in Fig. 6(b), the bleeding rate increased as the hydrostatic pressure increased in the initial stage.

With reductions in the sedimentation of aggregate particles and in free water due to the bleeding and the cement hydration, the hydrostatic pressure decreased gradually to a stable minimum value after it reached to a maximum value. This may be resulted from that the excessive pore water pressure decreased gradually and finally became to be zero. As the hydrostatic pressure decreased or became to be approximately a constant, the bleeding rate reduced gradually to zero (Fig. 6(b)).

When the concretes were vibrated, as shown in Fig. 7(a), measured water pressures increased with elapsed time and approached to a constant during the 5 minutes vibration, and they were smaller than those in the static state. These water pressures are considered to be excessive pore water pressures. Also, the bleeding rates increased with the vibration time.

Fig. 7(b) indicates the relationships between the excessive pore water pressure and the bleeding rate. We can find that the bleeding rate increased linearly with an increase in the excessive pore water pressure. It is concluded that the bleeding is due to the excessive pore water pressure.

4. CONCLUSIONS

An experimental investigation has been carried out to examine the bleeding behaviors and influencing factors for fresh concrete in standstill and vibrated states, respectively. Main conclusions have been drawn as follows.

- (1) A model shown in Eq.(4) is presented to describe the time-dependence of bleeding in static state, and the quantitative relationships between the parameters in the equation and the influencing factors such as specimen's dimensions were obtained, as shown in Table 3.

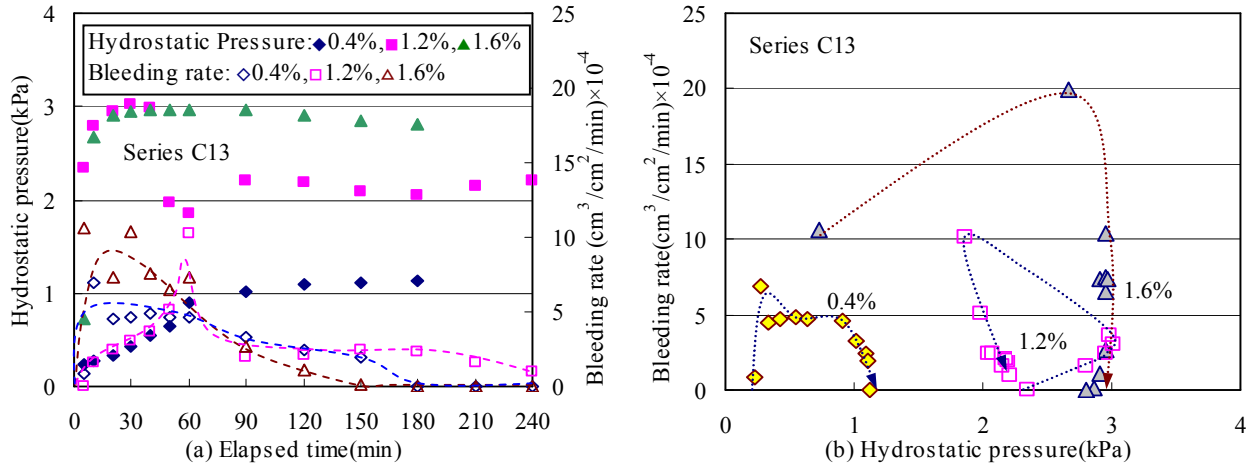


Fig. 6 Relationship between bleeding rate and hydrostatic pressure in standstill

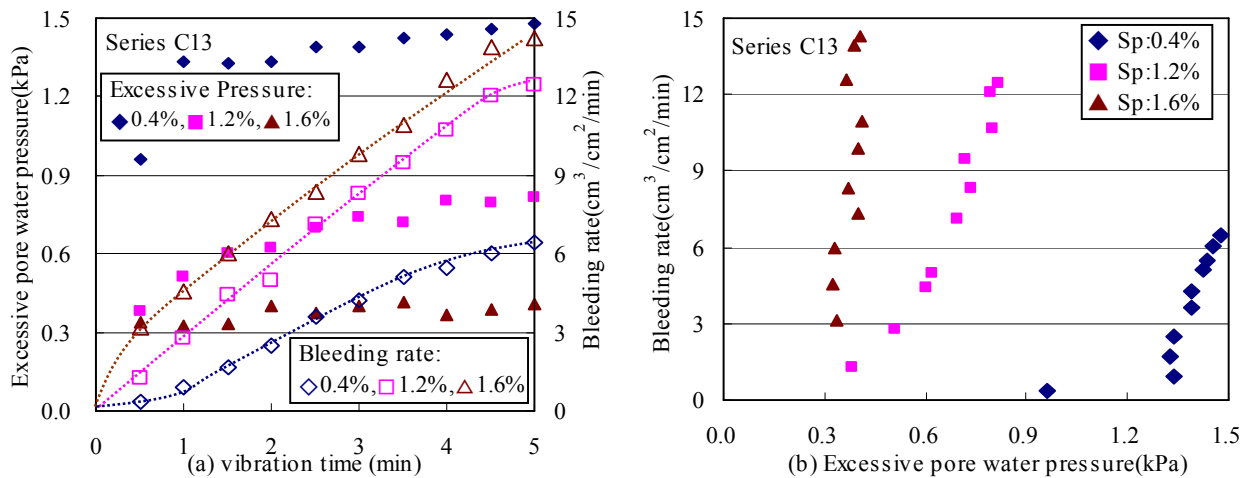


Fig. 7 Relationship between bleeding rate and hydrostatic pressure in vibration

- (2) The time-dependences of the bleeding capacities during vibration and after the vibration were also investigated. The relationships between the bleeding capacities in the standstill and during the 5 minutes vibration as well as during the whole process of the vibration plus standstill were examined quantitatively, as shown in Eqs. 5 and 6, and the effects of concrete's dimensions on these relationships were also discussed.
- (3) In static state, the bleeding rate first increased with time, then reduced gradually to zero after it reached to a peak value, as the hydrostatic pressure decreased or nearly kept a constant. However, in vibration process, excessive pore water pressure increased with time, and the bleeding rate increased linearly with an increase in the excessive pore water pressure.

The effect of vibration time on the relationship between the bleeding capacities in the static state and during the whole process of vibration plus standstill will be further investigated in the near future.

REFERENCES

- [1] P J Wainwright and H Ait-Aider, The influence of cement source and slag additions on the bleeding of concrete, *Cement and Concrete Research*, Vol.25, No.7, pp.1445-1456, 1995
- [2] Burak Felekoğlu, Selc-uk Türkel and Bülent Baradan, Effect of water/cement ratio on the fresh and hardened properties of self-compacting concrete, *Building and Environment*, Vol.42, pp.1795-1802, 2007
- [3] Yasumichi Kamisiro, Takesi Ooike and Tooru Kawaguchi, Bleeding characteristics of high fluidity concrete, *Japan Concrete Institute*, Vol.21, No.2, pp.445-450, 1999 (in Japanese)
- [4] Laurent Josserand, Olivier Coussy and François de Larrard, Bleeding of concrete as an ageing consolidation process, *Cement and Concrete Research*, Vol.36, pp.1603-1608, 2006
- [5] C.K. Loh, et al., An experimental study on bleeding and channelling of cement paste and mortar, *Advances in Cement Research*, Vol.10, No.1, pp.1-16, Jan., 1998
- [6] Chuichi Tashiro, et al., Water behavior in cement & concrete, Report of Water Sub-committee, *Research Committee of Cement & Concrete*, pp.152-153, Sep., 1994